

## Chlorination of niobium and tantalum ore

J. Gonzalez<sup>bc</sup>, F. Gennari<sup>ac</sup>, A. Bohé<sup>ac</sup>, M. del C. Ruiz<sup>bc</sup>, J. Rivarola<sup>bc</sup>, D.M. Pasquevich<sup>a,\*</sup>

<sup>a</sup> Comisión Nacional de Energía Nuclear (CNEA), Centro Atómico Bariloche (CAB), 8400-San Carlos de Bariloche, Río Negro, Argentina

<sup>b</sup> Instituto de Investigaciones en Química (INTEQUI), (5700) San Luis, Argentina

<sup>c</sup> Consejo Nacional de Investigaciones Científicas y Técnicas (CONICET), San Luis, Argentina

Received 6 May 1996; received in revised form 4 August 1997; accepted 10 August 1997

### Abstract

The reaction of chlorine with columbite concentrate, a niobium and tantalum ore, was studied by thermogravimetry between 300° and 950°C. Nonisothermal and isothermal measurements were performed. Morphological evolution of solid reactants and elemental composition of particles were analyzed by SEM and EDXS, respectively. The growth of crystals, high in Ta and Nb content, was observed. The Ta content in remaining samples was greater as the chlorination temperature increased. A scheme of the reaction mechanism is proposed. © 1998 Elsevier Science B.V.

*Keywords:* Chlorination mechanism; Columbite; Columbite chlorination; Niobium extraction; Tantalum extraction

### 1. Introduction

The direct reaction between Cl<sub>2</sub> and oxides of Nb and Ta for producing the respective chlorides is not thermodynamically feasible <1000°C. For this reason, the chlorination is performed in the presence of reducing agents, e.g. carbon [1], carbon monoxide [2,3], and so forth. Such chlorination reactions are of interest in the field of extractive metallurgy. In particular, the study of the chlorination of Nb and Ta oxides is related to the extraction of the respective metals [4–8]. However, the intrinsic mechanism of chlorination reactions has not been studied extensively [4–9]. Most of the studies have focussed on the analysis of the efficiency of chlorination for separating the chlorides from the remaining raw materials.

The reaction of chlorine alone with an ore of Nb and Ta components (called direct chlorination), even though thermodynamically unfavourable in equilibrium conditions, can progress until full conversion of the solid reactant is achieved when gaseous products are continuously removed. The study of this reaction is necessary for understanding elementary steps involved in more complex processes such as chlorination in the presence of carbon. However, the direct chlorination of Nb and Ta ores <1000°C has not been reported to the best of the authors' knowledge and direct chlorination of pure Nb<sub>2</sub>O<sub>5</sub> and Ta<sub>2</sub>O<sub>5</sub> has received only limited attention [9]. Gaballah et al. [9] have observed that the reactivity of Nb<sub>2</sub>O<sub>5</sub> towards chlorine is higher than that of Ta<sub>2</sub>O<sub>5</sub>. Moreover, they have suggested that direct chlorination of Nb<sub>2</sub>O<sub>5</sub> and Ta<sub>2</sub>O<sub>5</sub> can take place at low temperatures through an intermediate step involving the formation of NbO<sub>2</sub>Cl and TaO<sub>2</sub>Cl [9]. It has been reported that direct

\*Corresponding author. Tel.: 005494445269; fax: 005494445299; e-mail: pasquev@cab.cnea.edu.ar

chlorination of the mineral pyrochlore which contains niobium, involves the formation of various crystalline compounds [7,10]. Niobates of calcium, titanium and sodium were observed  $>1000^{\circ}\text{C}$  [7–10].

The present research was undertaken to obtain information of the fundamental processes taking place during the direct chlorination of an ore of Nb and Ta. A concentrate of a common mineral of Nb and Ta was chosen. It consists of mixed iron-manganese niobiantalates, with the general formula  $(\text{Fe,Mn})(\text{Nb,Ta})_2\text{O}_6$  [11,12]. The direct-chlorination of such a mineral was studied by thermogravimetry. Solid reactants at various steps of conversions were analyzed by SEM, EDXS and XRD.

## 2. Experimental

### 2.1. Materials

The raw oxide chosen for this study was an ore from San Luis, Argentina. The chemical composition of the concentrate, given as oxides, was:  $\text{Nb}_2\text{O}_5$  (41.2 wt%);  $\text{Ta}_2\text{O}_5$  (36.8 wt%);  $\text{TiO}_2$  (1.16 wt%);  $\text{MnO}$  (7.80 wt%);  $\text{FeO}$  (9.27 wt%);  $\text{SiO}_2$  (1.48 wt%);  $\text{Al}_2\text{O}_3$  (1.13 wt%) and others (1.13 wt%). The ore was crushed and ground to different particle sizes. Pure oxides of Nb (Fluka, AG, Buchs SG) and Ta (Fluka, AG, CH-9470 Buchs) were also used in order to compare the chlorine reactivity. The mineral and the pure oxides of Nb and Ta had a low BET surface area of 1.2, 1.55, and  $0.81\text{ m}^2/\text{g}$ , respectively.

### 2.2. Experimental procedure

The progress of reaction was studied by using a thermogravimetric system based on a Cahn electro-balance (Model 2000, Cahn) adapted for the use of chlorine. The measurements in such an experimental set-up under experimental conditions of this study have an accuracy of  $10\text{ }\mu\text{g}$ . More details of the thermogravimetric system and its performance have been given elsewhere [13].

Samples were placed in a quartz crucible and suspended within a vertical furnace and connected to the weighing unit by a quartz wire. Nonisothermal measurements were performed by heating samples from  $300^{\circ}$  to  $950^{\circ}\text{C}$  in a chlorine–argon mixture at

$P(\text{Cl}_2)=33\text{ kPa}$ . For isothermal runs, samples were brought to the desired reaction temperature under flowing argon. Chlorine gas was then injected and mass changes measured. Data were corrected for apparent mass changes [13]. Results were expressed as a fraction of mass loss  $(\Delta M/M_i)$ , where  $\Delta M$  represents the mass loss at time  $t$  and  $M_i$  the initial mass of the sample.

The ore and the reacted samples were analyzed by scanning electron microscopy (SEM), energy dispersive X-ray spectroscopy (EDXS) (SEM 515, Philips), XRD, X-ray diffraction (Rigaku D-MAX-IIIC), and X-ray fluorescence (XRF) (Philips PW 1400). The procedure has been described in detail elsewhere [14].

## 3. Results and discussion

### 3.1. Mineral characterization

From the aforementioned chemical composition, the formula of the Nb and Ta mineral is  $(\text{Mn}_{0.46}\text{Fe}_{0.54})(\text{Nb}_{0.65}\text{Ta}_{0.35})_2\text{O}_6$ , and is known as columbite. Fig. 1 illustrates morphological characteristics of a typical mineral particle corresponding to the fraction  $-200/+270$  mesh. The EDXS analysis performed on various particles is given in Table 1 for two sized fractions. The particles can be classified into two types: those of high Nb and Ta content (columbite particles) and those of high Si and Al content. High content of manganese and iron was always associated with Nb and Ta, while Na and K were mainly observed in high-silicon particles. It was also observed that

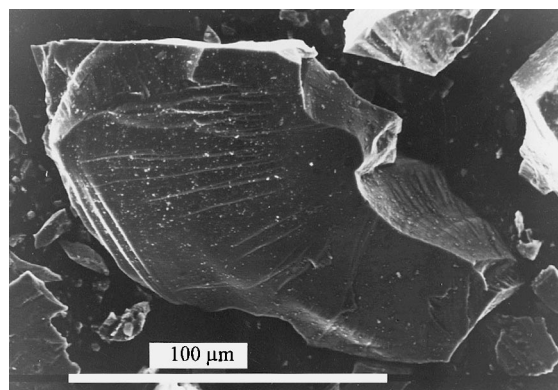


Fig. 1. Morphological and surface details of a typical particle of the mineral with high Ta and Nb content.

Table 1  
Analysis by EDXS of content elements composing particles of the mineral for two sized fractions, in atom %

Sized fraction (mesh)	Nb	Ta	Mn	Fe	Ti	Si	K	Na	Al	Ca
–100/+140	—	t <sup>a</sup>	t <sup>a</sup>	t <sup>a</sup>	—	98	t	—	1	—
–100/+140	3	t <sup>a</sup>	—	1	—	47	13	t <sup>a</sup>	34	1
–100/+140	43	16	17	8	t <sup>a</sup>	13	—	2	—	—
–100/+140	47	13	18	15	1	5	t <sup>a</sup>	—	—	t <sup>a</sup>
–200/+270	46	14	17	12	—	10	t <sup>a</sup>	—	—	—
–200/+270	56	7	6	20	—	11	—	—	—	—
–200/+270	—	t <sup>a</sup>	t <sup>a</sup>	2	—	45	17	t <sup>a</sup>	35	—

t<sup>a</sup> Traces (<1%).

there was no significant preferential concentration of Nb and Ta in the different sized fractions analyzed. The X-ray diffraction analysis of the ore, which will be given later on, revealed that particles with high silicon content were mainly mica (Si, Al and K containing particles) and quartz, while columbite pattern was well indexed by the orthorhombic structure (Fe<sub>0.52</sub>Mn<sub>0.48</sub>)(Nb<sub>0.68</sub>Ta<sub>0.32</sub>)<sub>2</sub>O<sub>6</sub> [15] which is in agreement with the chemical composition given here.

### 3.2. Thermodynamic considerations

The standard free-energy changes accompanying direct chlorination of most of the mineral constituents considered as oxides are shown in Fig. 2. The plot

allows one to compare chlorine reactivity with each oxide. The formation of chlorides does not take place spontaneously in the 400–1000°C range, except for a few oxides. The values of  $\Delta G^0$  for the reactions involving the formation of chlorides of Nb and Ta are highly positive throughout the temperature range analyzed. The same observation is valid for the chlorination of Al<sub>2</sub>O<sub>3</sub> and SiO<sub>2</sub>. On the other hand, the values of  $\Delta G^0$  for the chlorination of FeO, and MnO are negative. Therefore, chlorination of these oxides and production of the respective chlorides is thermodynamically feasible.

Tantalum oxide on chlorination gives only TaCl<sub>5</sub> [11,12]. On the contrary, the chlorination of Nb<sub>2</sub>O<sub>5</sub> can produce NbOCl<sub>3</sub>, as reported by different authors

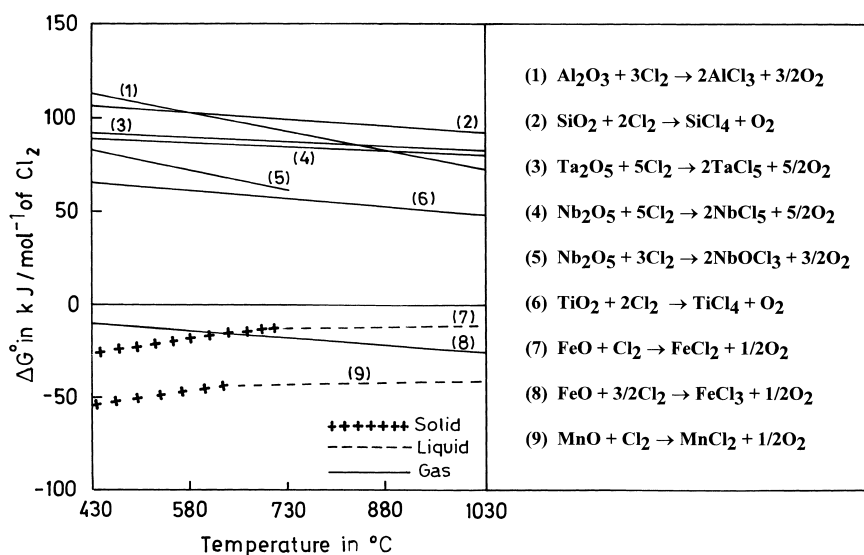


Fig. 2. Values of Gibbs free-energy change ( $\Delta G^0$ ), in kJ/mol of Cl<sub>2</sub>, for several reactions between chlorine and various metallic oxides. Stable states are also indicated.

[11,12]. The oxychloride is thermodynamically favoured as compared to the respective chloride, as shown in Fig. 2.

Fig. 2 also shows the stable states of the different reaction products. Above 400°C, all the chlorides are practically gases with the exception of FeCl<sub>2</sub> and MnCl<sub>2</sub>. The iron chloride sublimes >640°C and the MnCl<sub>2</sub> melts at 650°C. The respective vapour pressures are given by the following expressions [16]:

$$\log P(\text{FeCl}_2, \text{kPa}) = -9475T^{-1} - 5.23 \log(T) + 25.65$$

$$\log P(\text{MnCl}_2, \text{kPa}) = -10606T^{-1} - 4.33 \log(T) + 22.8$$

For instance, the vapour pressure of FeCl<sub>2</sub> is 0.75, 14 and 57 kPa at 650°, 830° and 950°C, respectively. At these temperatures the values for MnCl<sub>2</sub> are 0.03, 1 and 6 kPa, respectively.

### 3.3. Chlorination of the niobium and tantalum ore concentrate

The overall composition of the mineral indicates that ca. 82 wt% corresponds to oxides with a high thermodynamic stability in chlorine atmosphere, as shown in Fig. 2. In fact, chlorination reactions of oxides of Nb, Ta, Ti, Al and Si have very positive standard free-energy changes. On the other hand, direct chlorination of Mn and Fe oxides is thermodynamically feasible. Table 1 indicates that iron and manganese were always present in the particles of high Nb and Ta content, which is in agreement with the fact that Fe(II) and Mn(II) occupy positions of the iron-manganese niobiotantalates. Consequently, the chlorination of Fe and Mn causes the chemical disruption of the columbite particles to occur.

Nevertheless, mass loss is observed in the non-isothermal chlorination of the mineral. In effect, Fig. 3 shows the thermogravimetric curves between 300° and 950°C for two sized fractions: -200/+270 and -325 mesh. It is noticed that the mass loss and, therefore, the ore chlorination, started at ca. 500°C for the -325 mesh sized fraction, and at ca. 590°C for the other sized fraction (-200/+270 mesh). The greater conversion was achieved for smaller particles (ca. 0.23 at 950°C) which is probably a consequence of a higher specific surface area.

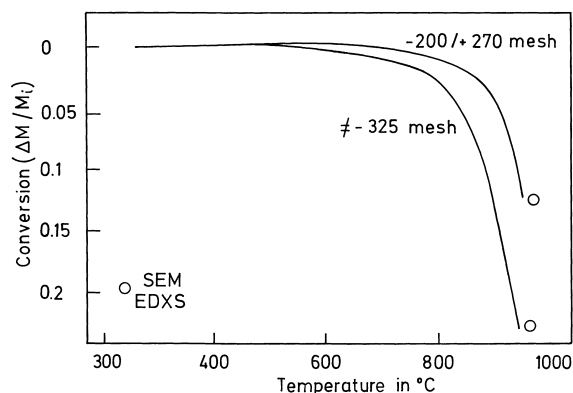


Fig. 3. Non-isothermal chlorination of the mineral for two sized fractions.

Among chlorides indicated in Fig. 2, those of Fe and Mn are the most likely to be formed. Therefore, mass loss at ca. 500–600°C is mainly attributed to the volatilization of Fe as FeCl<sub>3</sub>, which is gaseous >315°C, and Mn as MnCl<sub>2</sub>, which may be eliminated from the reaction bed >650°C. The formation of these chlorides indicates that a chemical disruption of the structure of the columbite particles occurred as indicated here.

In order to understand the type of chemical attack, reacted samples were analyzed by SEM and EDXS at those conversions indicated in Fig. 3. Particles with crystals grown on their surfaces were observed, as shown in Fig. 4(a) and (b) (to compare with Fig. 1). Two different types of crystals are noticed: type I crystals of rounded shape, Fig. 4(a), and type II crystals of acicular shape, Fig. 4(b). The elemental compositions of type I and II crystals and the particle surface (PS) are given in Table 2. Type I crystals were high in Nb and Ta, with a greater content of the latter. Besides Nb and Ta, type II crystals had Ti, Mn and Fe. Analyses of particle surfaces on which crystals apparently have grown indicated similar elemental composition to that observed for the ore particles before chlorination.

Crystals of type I and II were only observed on reacted columbite particles. Neither crystals nor chemical attack were observed on high-silicon particles. The high concentration of Nb and Ta observed in both types of crystals, which was greater than in the ore particle, suggests that the chlorides of Fe and Mn were volatilized during chlorination. Moreover, the signal

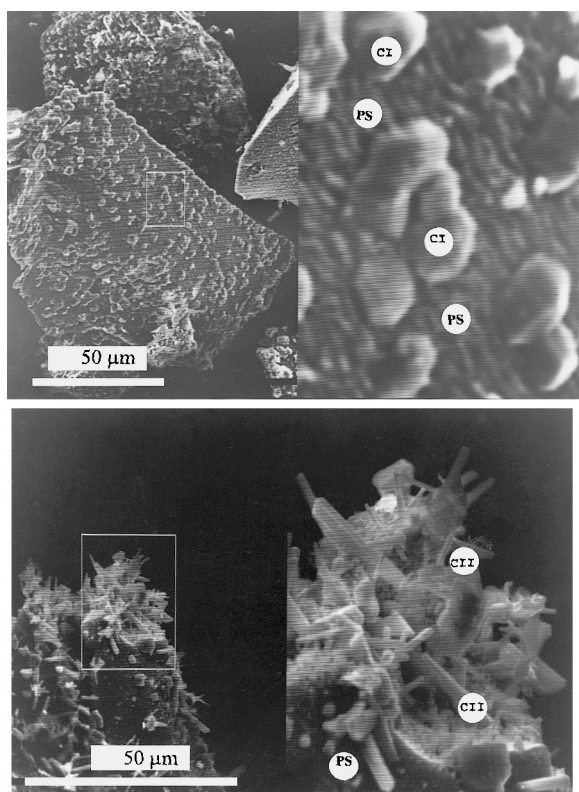


Fig. 4. (a) Microphotography of raw oxide particle showing the formation of rounded crystals (CI) on its surface. Sample from  $-200/+270$  mesh fraction. (b) Microphotography of raw oxide particle showing the formation of acicular crystals (CII) after chlorination of the  $-325$  mesh sample.

of CI was not detected by EDXS in the samples analyzed at  $950^{\circ}\text{C}$ . Therefore, the selective elimination of Fe and Mn is in agreement with their stable states as chlorides and vapour pressures, as indicated in the foregoing.

As a result, mass loss and crystal formation observed in nonisothermal chlorination demonstrate that ore particles react with chlorine to form both, gaseous and solid products. Gaseous products are mainly Fe and Mn chlorides, and crystals are mainly oxides of high Nb and Ta content (see EDXS analysis, Table 2). The crystal formation is certainly a complex process, which may involve both, solid recrystallization and gaseous-solid interactions. Solids may react through a multi-step process accompanied by recombination of gaseous products and formation of intermediate compounds [17,18]. Crystals of type I and II are a consequence of such a multi-step process. Crystals of type I are probably formed by a solid reaction product recrystallization. In the case of crystals of type II, there may occur both, solid recrystallization and solid-gas interactions, the latter being favoured by the slow removal rate of gaseous products into the argon-chlorine flow in thermogravimetric runs. In fact, gas-solid interaction between gaseous and solid products cannot be disregarded.

Actually, this effect has been observed in  $\text{TiO}_2$  chlorination, where the gaseous products underwent the reverse reaction forming huge faceted  $\text{TiO}_2$  crys-

Table 2

(a) Elemental composition of partially chlorinated particles and crystals formed during the ore chlorination (nonisothermal), in atom%. Crystals of types I and II and particle surface are denoted by CI, CII, and PS, respectively

$T^a$ ( $^{\circ}\text{C}$ )	$X^b$ (%)	Figure	Analyzed region	Nb	Ta	Ti	Mn	Fe
950	12	4a	CI	48	52	—	—	—
			CI	43	57	—	—	—
			CI	48	52	—	—	—
			PS	48	18	3	22	9
			CI	49	51	—	—	—
			PS	29	33	2	25	11
			CI	58	39	2	1	—
950	23	4b	PS	62	15	2	16	5
			CII	55	26	9	7	3
			PS	56	14	2	19	9
			CII	57	26	8	5	4
			PS	63	10	2	17	8

$T^a$  Temperature.

$X^b$  Conversion.

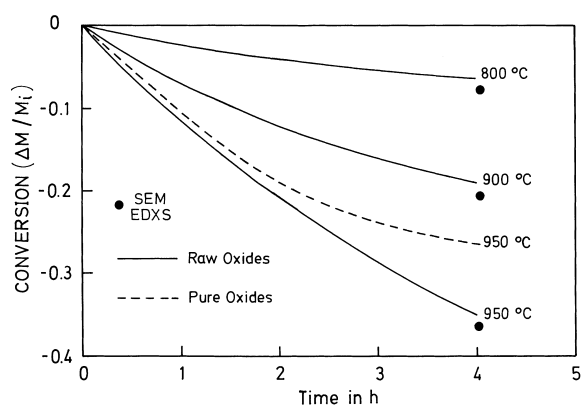


Fig. 5. Effect of temperature on the chlorination of the mineral. For comparison, the chlorination of a mixture of pure oxides of Nb and Ta at 950°C is also shown.

tals with the typical crystalline habit of rutile [19,20]. The partial pressure of  $\text{TiCl}_4$  in those experiments was 0.35 kPa. Hence, it is possible that during the ore chlorination, chlorides of Nb and Ta, which are metastable, deposit Nb and Ta oxides on unreacted ore particles due to the reaction that may occur between  $\text{O}_2$  and  $\text{TaCl}_5$  and  $\text{O}_2$  and  $\text{NbOCl}_3$ . The possibility of crystal growth from gaseous phase is supported by big faceted crystals deposited on partially reacted ore particles shown in Fig. 6, which will be discussed later.

In order to improve the understanding of the reaction path, isothermal chlorination of the ore and of a mixture of pure  $\text{Ta}_2\text{O}_5$  and  $\text{Nb}_2\text{O}_5$  with a 1/1 ratio were

performed. The mixture of pure oxides, of similar BET area and particle-size distribution as that of the mineral, was less reactive than the raw oxides at 950°C (Fig. 5). The temperature had a strong effect on the chlorination rate of the ore. The conversion was about 35% at 950°C, 20% at 900°C and 5% at 800°C in the same reaction time (4 h). Reacted samples were analyzed by SEM, EDXS, XRD and XRF at various conversions. In all these samples, crystal growth was observed. At 800° and 900°C, the size and form of the crystals were similar to those shown in Fig. 4(b). The composition of acicular crystals was of high Ta and Nb content as indicated in Table 3. At 950°C, large crystals (Fig. 6), mainly formed by Nb and Ta, were observed. Table 3 indicates that iron was barely observed in the crystals and the Mn concentration was noticeably lower than that of crystals of Fig. 4(a and b). The big size of the crystals of Fig. 4(b) is in agreement with the highest conversion achieved at 950°C. It is concluded that as temperature and conversion increase, the crystal growth is greater and, thus, chlorination upgrades the mineral in crystals of Nb and Ta oxides. Consequently, as chlorination of the ore progresses the residue is less reactive, which is in agreement with the lower reactivity of pure oxides shown in Fig. 5.

In the zone indicated by the circle in Fig. 6 a high concentration of Fe and Mn was observed, which is in agreement with the content of the elements in the starting particles. However, the particle surface shows corrosion as inferred from a comparison with starting

Table 3  
Elemental composition of particles and crystals formed during the ore chlorination under isothermal conditions, in atom %

$T^a$ (°C)	$X^b$ (%)	Figure	Analyzed region	Nb	Ta	Ti	Mn	Fe
800	5		CII	27	67	3	—	3
			CII	25	65	1	—	9
900	18		CII	42	49	9	—	—
			CII	45	42	13	—	—
			CII	51	41	8	—	—
950	35	6	arrow	51	47	2	$t^c$	—
			arrow	48	48	3	$t^c$	—
			circles	60	13	2	18	7
			arrow	31	65	3	$t^c$	$t^c$

$T^a$  Temperature.

$X^b$  Conversion.

$t^c$  Traces (<1%).

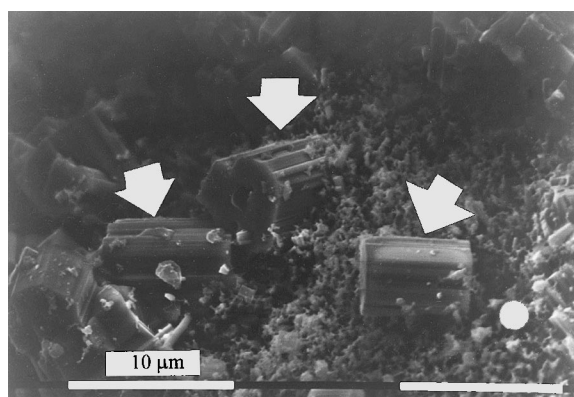


Fig. 6. Residue of an isothermal chlorination experiment (ca. 35% conversion) performed at 950°C. Arrows, which show big crystal, and circles indicate places where analyses by EDXS were performed.

particles shown in Fig. 1. The observed zone shows the chemical attack of chlorine, which may take place at the grain boundaries or imperfections of the particle surface. Considering that EDXS analysis indicates absence of Cl, chlorides of Fe and Mn were probably volatilized as soon as they were formed at 950°C. This is also supported by data of Table 3 since the big crystals (arrows in Fig. 6), grown from gaseous phase, have a low content of Fe and Mn.

Table 3 shows that all the crystals have a Ta/Nb ratio of  $\approx 1/1$ , which is greater than that for starting particles, i.e. a Ta/Nb ratio of ca. 0.3 in Table 1. Hence, it is concluded that direct chlorination upgraded the crystals in Ta. The Ta increase is also verified in the bulk chemical composition of the residues, as determined by X-ray fluorescence analysis. Table 4 summarizes ore, Nb and Ta conversions at various temperatures. The data show that when the ore chlorination achieved a 16.5% mass loss, 28% of Nb

Table 4  
Ore, Nb and Ta conversions at various temperatures

Temperature (°C)	Ore conversion <sup>a</sup> (%)	Nb conversion <sup>b</sup> (%)	Ta conversion <sup>2</sup> (%)
800	16.5	28	0
900	26.4	45	1.0
950	32.3	53	3.5

<sup>a</sup> As determined by thermogravimetry.

<sup>b</sup> As determined by XRF analysis in the solid residues.

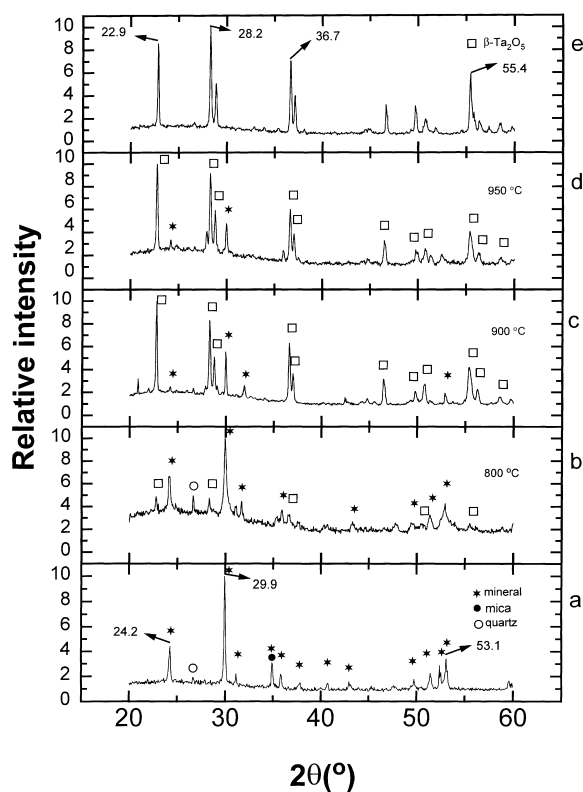


Fig. 7. Patterns of X-ray diffraction. (a) – mineral; (b–d) correspond to reacted sample at 800°C – conversion 5%, at 950°C – conversion 35%, and at 1000°C – conversion 65%, respectively; and (e)  $\beta$ -Ta<sub>2</sub>O<sub>5</sub>.

had evolved as gaseous products while all Ta remained in the solid residue. Thus, it is assumed that the mass loss at 800°C is mainly due to the formation of FeCl<sub>3</sub>, MnCl<sub>2</sub>, O<sub>2</sub> and NbCl<sub>5</sub> and/or NbOCl<sub>3</sub>. At higher temperatures, 900° and 950°C, the ore chlorination also evolved toward a solid residue rich in Ta. In fact, the amount of Ta evolving as gaseous product is solely 1% at 900°C and 3.5% at 950°C, which contrasts with the higher Nb conversion, i.e. 45 and 53%, respectively.

In order to identify the solid residue rich in Ta, XRD analysis of the residues of Fig. 5 was performed. Fig. 7 shows the diffraction lines of the corresponding X-ray patterns at 800°C (Fig. 7(b)), 900°C (Fig. 7(c)) and 950°C (Fig. 7(d)), with an ore conversion, i.e. mass loss of 5, 18 and 35%. For the purpose of comparison, the patterns of the starting mineral (Fig. 7(a)) and pure Ta<sub>2</sub>O<sub>5</sub> phases (Fig. 7(e)) are also

shown. The pattern of the mineral indicates the typical lines of niobiantantalates of Fe and Mn which correspond to  $2\theta=29.9^\circ$ ,  $24.2^\circ$  and  $52.9^\circ$ . The typical diffraction lines of quartz and mica were also observed, at  $2\theta=26.7^\circ$  and  $34.9^\circ$ , respectively. It is noticed that after chlorination, the two most intense lines of the niobiantantalate are also observed at  $800^\circ$ ,  $900^\circ$  and  $950^\circ\text{C}$ , which indicates the presence of unreacted mineral. At  $950^\circ\text{C}$  (Fig. 7(d)), the lines at  $2\theta=29.9^\circ$  and  $24.2^\circ$  decreased significantly, which is in agreement with the high conversion of the mineral.

At  $800^\circ\text{C}$ , lines at  $2\theta=28.2$ ;  $22.9$ ;  $36.7$  and  $55.4$ , corresponding to a new solid phase formed during chlorination are also observed. The intensity of these lines increases with temperature and conversion (Fig. 7(c and d)). Also other less intense diffraction lines appear at  $900^\circ$  and  $950^\circ\text{C}$ . All these lines can be understood on the basis of the formation of an orthorhombic structure type  $\beta\text{-Ta}_2\text{O}_5$ . A comparison of the patterns of this oxide (Fig. 7(e)) with those corresponding to partially chlorinated samples (Fig. 7(b–d)) clearly supports this conclusion. At  $950^\circ\text{C}$ , the residue with a high conversion (Fig. 7(d)) shows that the remaining sample is practically  $\beta\text{-Ta}_2\text{O}_5$ , which probably has Nb in its structure, due to the high tendency of Nb and Ta to form solid solutions [11,12]. Accordingly, the columbite chlorination upgrades the mineral in  $\text{Ta}_2\text{O}_5$ .

### 3.4. Mechanism of columbite chlorination

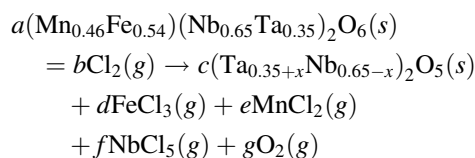
The experimental results indicate that the ore chlorination proceeds with the formation of gaseous chlorides of Fe and Mn and with a preferential chlorination of Nb with respect to Ta. The formation of Nb is readily demonstrated by the chemical analysis performed on residues at various conversions, as summarized in Table 4. Although Fig. 2 shows that  $\text{Nb}_2\text{O}_5$  chlorination, in equilibrium conditions, is thermodynamically unfavourable, chlorination is possible due to the fact that gaseous products are continuously removed with the  $\text{Ar-Cl}_2$  flow used in the thermogravimetric runs presented in this paper. The preferential chlorination of Nb with respect to Ta can be understood on the basis of the different thermodynamic stabilities of the respective oxides. In fact, Fig. 2 shows that  $\text{Nb}_2\text{O}_5$  chlorination through reactions 4 and 5, which have a lower Gibbs free-energy

change, is more probable than reaction 3, which corresponds to  $\text{Ta}_2\text{O}_5$  chlorination.

The selective  $\text{Nb}_2\text{O}_5$  chlorination is also in agreement with a recent study reported by Gaballah et al. [21]. These authors have demonstrated that the chlorination of a rich concentrate containing ca. 60% of  $\text{Ta}_2\text{O}_5$  and  $\text{Nb}_2\text{O}_5$  oxides proceeds with an increase in tantalum oxide content as the temperature rose, while that of  $\text{Nb}_2\text{O}_5$  shows a decrease. Those results were confirmed from measurements of the Ta/Nb ratio, which varied from 1.23 (initial content) to 2.27 at  $1000^\circ\text{C}$  (mass loss 73 wt%).

Based on the findings of this investigation the following reaction scheme illustrates the ore chlorination:

**Step 1:** The first step of ore chlorination is the chemical disruption of columbite particles to form gaseous and solid products. The first ones are mainly composed by  $\text{FeCl}_3$  and  $\text{MnCl}_2$  and minor amounts of  $\text{NbCl}_5$  and/or  $\text{NbOCl}_3$  and  $\text{O}_2$ . The solid products consist of crystals of high Ta and Nb content. To illustrate the overall process the following general equation can be proposed:



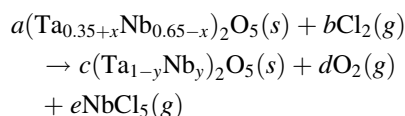
where the general stoichiometric coefficients ( $a, b, \dots, g$ ), depend upon the  $x$  value. The general formula  $(\text{Ta}_{0.35+x}\text{Nb}_{0.65-x})_2\text{O}_5$  (with  $0 \leq x \leq 0.65$ ), represents the formation of crystals of type I and II. As shown in Table 2, these crystals have variable composition (represented by  $x$  in the foregoing general formula), which is in agreement with the fact that  $\text{Nb}_2\text{O}_5\text{-Ta}_2\text{O}_5$  solid solutions are possible over a wide range of composition [22].

Thus, Step I, which takes place  $>500^\circ$  or  $590^\circ\text{C}$ , depending on the sized fraction, as shown in Fig. 3, indicates that the chlorination upgrades the ore in order to produce particles of high Nb and Ta content, as supported by elemental composition of crystals of type I and II.

**Step 2:** At higher temperatures and greater conversions, the reacted residue is upgraded in Ta. For



instance, the following reaction illustrates the probable process:



where the general formula,  $(\text{Ta}_{1-y}\text{Nb}_y)_2\text{O}_5$  emphasizes that the chlorination evolved towards an orthorhombic structure of  $\beta\text{-Ta}_2\text{O}_5$  which probably has  $\text{Nb}^{5+}$  in the lattice. Following the literature [23], the orthorhombic structure is valid for  $0 \leq y \leq 0.5$ . Thus, the general stoichiometric coefficients depend on the  $x$  and  $y$  value. For instance  $a=1.8$ ,  $b=2.5$ ,  $c=1.3$ ,  $d=1.25$  and  $e=1$ , when  $x=0.3$  and  $y=0.1$ .

Although the XRD analysis shown in Fig. 7 supports the formation of the orthorhombic structure of  $\beta\text{-Ta}_2\text{O}_5$ , the formation of a  $\beta\text{-Ta}_2\text{O}_5$  solid solution is highly probable in view of the close similarity between the size of  $\text{Nb}^{5+}$  and  $\text{Ta}^{5+}$  ions. For this reason, Step II indicates the formation of  $(\text{Ta}_{1-y}\text{Nb}_y)_2\text{O}_5$  with the proviso that the amount of Nb within the  $\beta\text{-Ta}_2\text{O}_5$  lattice may be variable.

#### 4. Summary

The chlorination rate of Ta and Nb ore, columbite, was found to be faster than that of pure oxides. Direct chlorination became significant  $>500^\circ\text{C}$ . The reaction involves breakdown of the structure of the columbite particles. Chlorides of Fe and Mn were volatilized and crystals high in Nb and Ta content were grown from the gaseous phase. The chlorine reactivity of the mineral decreased with conversion due to the fact that the residue was rich in Nb and Ta oxides. At high temperatures and high conversions, the residue composition mainly became rich in  $\text{Ta}_2\text{O}_5$ .

#### References

- [1] F. Fairbrother, A.H. Cowley, N. Scott, *J. Less-Common Metals* 1 (1959) 206.
- [2] L. Freitas, F. Ajersch, *Chem. Eng. Comun.* 30 (1984) 19.
- [3] I. Gaballah, E. Allain, M. Djona, *Min. Met. Mat. Soc.* (1992) 759.
- [4] C.K. Gupta, P.K. Jena, *Trans. Indian Metals* 18 (1965) 89.
- [5] A.W. Henderson, S.L. May, K.B. Higbie, *Ind. Eng. Chem.* 50(4) (1958) 611.
- [6] F. Habashi, I. Malinsky, *Can. Min. Metall. Bulletin* 69(766) (1976) 1.
- [7] P. Menbus, *Metall. Trans.* 10B(1) (1979) 93.
- [8] A.W. Henderson, *J. of Metals* 16(2) (1964) 155.
- [9] I. Gaballah, E. Allain, M. Djona, *Light Metals* 1 (1994) 153.
- [10] R. Berjoan, P. Menbus, *Metall. Trans.* 8B (1977) 461.
- [11] J.D. Gilchrist, *Extraction Metallurgy*, Pergamon Press, Oxford, 1980, p. 380.
- [12] C.A. Hampel, *Rare Metals Handbook*, Reinhold Publishing Corporation, New York, 1954.
- [13] D.M. Pasquevich, A. Caneiro, *Thermochim. Acta* 156 (1989) 275.
- [14] M. del C. Ruiz, J. González, R. Olsina, *J. Chem. Tech. Biotechnol.* 57 (1993) 375.
- [15] Card number 33-659. JCPDS, Powder Diffraction File, 1995.
- [16] O. Kubaschewski, E. Evans, C. Alcock, *Metallurgical Thermochemistry*, Pergamon Press, Oxford, 1967.
- [17] L. Stoch, *Thermochim. Acta* 148 (1988) 149.
- [18] L. Stoch, *J. Thermal Analysis* 40 (1993) 107.
- [19] J. Andrade Gamboa, D.M. Pasquevich, *J. Amer. Ceram. Soc.* 75(11) (1992) 2934.
- [20] M.J. Readey, D.W. Readey, *J. Amer. Ceram. Soc.* 69(7) (1986) 580.
- [21] I. Gaballah, E. Allain, M. Djona, *Proceeding of EPD Congress, Minerals Metals and Materials Society*, 1992, p. 759.
- [22] M. Zafrir, A. Aladjem, R. Zilber, L. Ben-Dor, *J. Solid State Chem.* 18(4) (1976) 377.
- [23] F. Holtzberg, A. Reisman, M. Berry, M. Berkenblit, *J. Amer. Chem. Soc.* 79(5) (1957) 2039.